

## CENTRAL CHILE SEISMOTECTONICS AND STRESS DISTRIBUTION ALONG THE SUBDUCTED NAZCA PLATE (25°-40°S)

Mario PARDO<sup>(1)</sup>, Diana COMTE<sup>(1)</sup>, Tony MONFRET<sup>(1,2)</sup>, Emilio VERA<sup>(1)</sup> and Nelson GONZALEZ<sup>(1)</sup>

<sup>(1)</sup>Departamento de Geofísica, Universidad de Chile. Casilla 2777, Santiago, Chile.

<sup>(2)</sup>Mission ORSTOM, Román Dfáz 264, Santiago, Chile.

**KEY WORDS:** Nazca Plate, Subduction, Seismotectonics, Stress Distribution, Central Chile.

### INTRODUCTION

The seismicity and tectonic of central Chile is mainly characterized by the subduction of the oceanic Nazca plate beneath the continental South American lithosphere. The rate of convergence between these two plates is relatively constant within the studied region due to the distant location of their rotation pole. This convergence rate is about 8.4 cm/yr in the N78°E direction [1].

Several studies have shown that the shape of the oceanic downgoing slab in the region, exhibits lateral variations in the dip [2,3,4]. Major changes in dip had been interpreted as segmentation of the downgoing slab bounded by tears or by continuous flexure of the slab. Based on teleseismic locations, the boundaries between these segments have been interpreted as tears in the oceanic slab [2,5]. In Chile-western Argentina, a continuous contortion of the slab around 33°S has been proposed [4,6,7]. Beneath the latitudes 28°-33°S, the subducted Nazca plate extends eastward in an almost subhorizontal trajectory for hundreds of kilometers at a depth of ~100 km before reassuming its downward descent [4,7]. These investigations are mainly focused around the principal changes in dip and there are no detailed studies south of 34° S, where the seismicity level is lower than in other regions of Nazca plate.

In this study, we improve the local and teleseismic hypocenter locations and determine new focal mechanisms, which along with those reported within the region permit a better analysis of the seismotectonic characteristics of central Chile relative to the shape of the subducted Nazca plate, the associated stress field and the geometry of the interplate coupled zone.

### LOCAL AND TELESEISMIC DATA

The data used in this study are accurately determined hypocenters obtained from local data recorded by seismological stations at the zone and from events recorded at teleseismic distances by the world wide seismological network, which were relocated using the method of Joint Hypocenter Determination (JHD) [8]. Focal mechanisms of 18 events that occurred between 1980 and 1987, were determined using body wave inversion [9] of the long-period P, SH and SV wave forms recorded at teleseismic distances ( $25^\circ \geq \Delta \geq 90^\circ$ ) by the Global Digital Seismograph Network. Focal mechanisms reported by other authors were also used.

Accurate hypocenters of local earthquakes were determined using data from the permanent telemetric network of the University of Chile since 1980 (32.7°-34.6°S) and from temporary networks deployed in the zone in 1985 (32.9°-34.5°S), 1986 (32.4°-33.7°S) and 1995 (34.0°-35.5°S).

Earthquakes with magnitude  $m_b \geq 4.8$  recorded at teleseismic distances, were relocated in central Chile with the JHD method [8], using the phase readings reported by the International Seismological Centre (ISC) between 1964 and 1994. The calibration events used in this relocation correspond to 15 earthquakes locally recorded and focal depths constrained by the body-wave inversion. The reason to relocate hypocenters from teleseismic data is the observed mislocation between the hypocenters reported by the international agencies (ISC, NEIC) and the ones determined with local data. On average, this mislocation results to be of  $\sim 10$  km in the  $N67^\circ E$  direction, but in many cases this mislocation can exceed 20 km.

## DISCUSSION

The epicentral distribution of the accurately located local and teleseismic events is presented on Figure 1. To analyze the geometry and state of stress of the subducted slab, eight cross-sections of the seismicity, including focal mechanisms, were drawn (Figure 2). The cross-sections are oriented in the direction of convergence between the Nazca and South American plates [1], and their origins coincide with the trench axis.

The shallow part of the subduction zone indicates a constant interplate geometry, under a compressional stress regime, that initially dips  $\sim 10^\circ E$  and gradually increases to  $\sim 25^\circ E$  at a depth of  $\sim 60$  km (Figure 2). This geometry is observed throughout the subduction zone in central Chile, and appears to be independent of the age and relative convergence rate of the interacting plates. No lateral changes of the interplate geometry are observed at places where major bathymetric features are subducted, as the Juan Fernandez Ridge (JFR) around  $33^\circ S$  (Figure 1).

The depth extent of the seismogenic interplate contact can be estimated from the maximum depth of the shallow thrust earthquakes and the depth of transition between compressional to tensional events [10]. This depth is  $\sim 60$  km throughout the studied zone of central Chile, in agreement with previous results on selected places along the Chilean subduction zone [10,11,12]. This result yields a maximum seismogenic width of 145 km, assuming an average dip of the subducted slab of  $20^\circ$  and considering that the slab is aseismic at the first 10 km from the trench.

The subducted Nazca plate shows lateral variations in the dip angle at depths greater than 60 km, where the stress regime is tensional (Figure 2). The seismicity pattern at these depths defines two regions within the downgoing slab bounded by the inland projection of the JFR, which is parallel to the convergence direction (Figure 1):

(1) A northern region, where the seismicity defines a Wadati-Benioff zone with variable dip, from  $\sim 30^\circ E$  (Figure 2A) to a gradually shallower dip to the south, where the slab becomes almost subhorizontal underplating the continental crust between latitudes  $28^\circ S$  and  $33^\circ S$  at depths of  $\sim 100$  km (Figures 2C, 2D). The seismicity is well observed down to depths of 200 km, from where a void in seismicity is present until depths between 550 and 600 km, where the plate is again seismic active (Figures 2A, 2B, 2C). If no detachment of the Nazca plate is assumed, the slab is sharply bended around depths of 200 km and then it sinks into the mantle with an almost constant dip of  $\sim 45^\circ$ , with seismicity that reaches to maximum depths of 600 km.

(2) A southern region, where the seismicity is more scarce and defines a Wadati-Benioff zone that reaches maximum depths  $< 200$  km, at closer distances from the trench than in the northern region (Figures 2E, 2F, 2G, 2H). The deep seismicity observed at depths between 550 and 600 km in the northern region, disappears in this region.

Back-arc crustal shallow seismicity occurs mainly in the zone of subhorizontal geometry of the downgoing Nazca plate. This geometry permits to transfer compressional stress to the overriding plate and inhibits the presence of a mantle wedge, so there are no active volcanoes over this zone (Figures 2C, 2D). Outside this zone, the active Quaternary volcanoes are well developed and they are located over the zone where the Nazca plate reaches depths of  $\sim 100$  km.

A sharp flexure in the slab occurs around  $33^\circ S$ , with strike parallel to the convergence direction between the interacting plates. The intersection of the JFR with the trench near latitude  $33^\circ S$ , which is

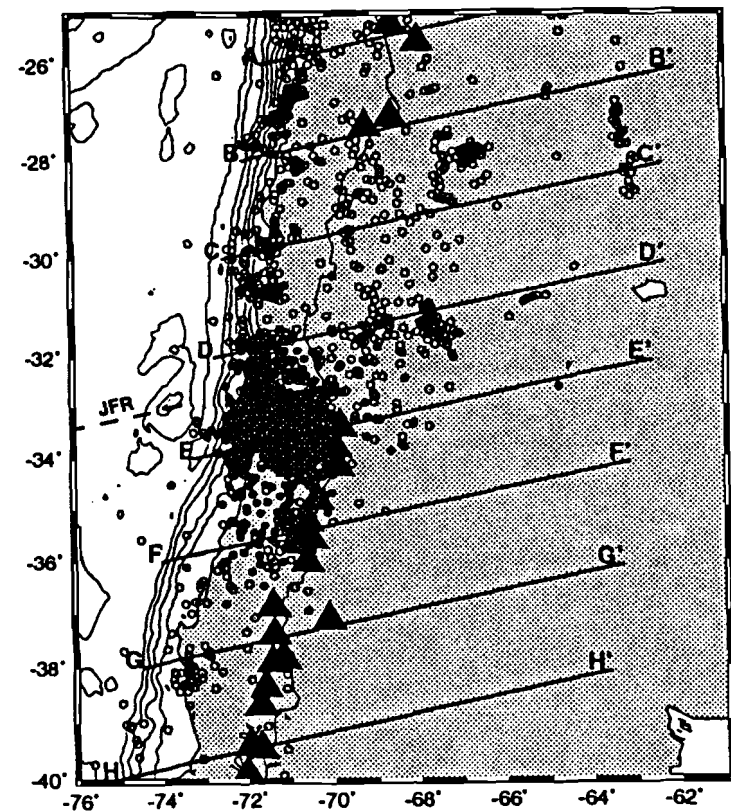


Figure 1.- Epicenters of the earthquake dataset used in this study from local data (solid circles) and from teleseismic data (open circles). The locations of the cross-sections of Figure 2, the Quaternary volcanoes in the zone (solid triangles) and the projection of the JFR (dashed line) are also shown.

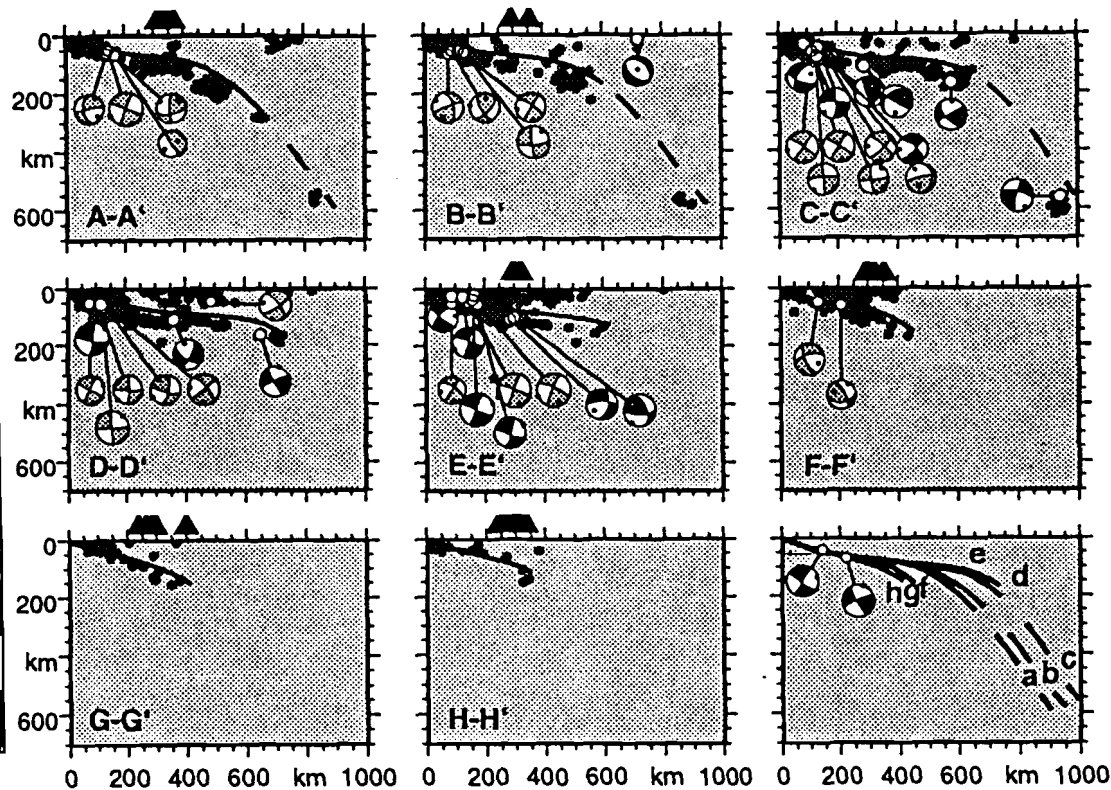


Figure 2.- Cross-sections of the relocated seismicity of Figure 1. The origin is at the trench and oriented in the convergence direction ( $N78^{\circ}E$ ). Focal mechanisms determined in this study (black) and reported from wave inversion (grey) are presented on a side-looking, lower hemispheric projection. The top of the downgoing oceanic Nazca plate is shown on each cross-section with a solid line; a dashed line is shown where it is interpolated. The location of Quaternary volcanoes (black triangles) are also projected at the top of each cross-section. At the right bottom, a summary of the Wadati-Benioff zone observed in each cross-section is presented.

located at the northern edge of the Challenger Fracture Zone, implies that lithospheric plates of different ages are subducted, being younger to the south of this boundary

## CONCLUSIONS

These observations suggest an older segment of the Nazca plate to the north of the projection of the JFR at 33°S, which sinks into the mantle down to depths of 600 km and bends probably due to gravitational forces. Between latitudes 28°S and 33°S however, at intermediate depths (60-100 km) the slab flattens and moves upwards probably related to the subduction of buoyant lithosphere associated to the the JFR. To the south of 33°S, a younger and shorter Nazca plate is suggested.

The observed stress pattern shows compression at shallow depths (<60 km) related to the coupled plate interface between the oceanic and the continental overriding plates. Downdip, at depths greater than 60 km, the downgoing plate is under tensional stress regime with T-axes oriented, in general, along the direction of the subducted oceanic plate.

The subhorizontal geometry of the subducted Nazca plate between 28°S and 33°S, at depths less than 100 km and distances from the trench between 200 and 500 km, may be responsible of the absence of Quaternary volcanism, the crustal shortening of the Andes and the associated back-arc crustal seismicity in Argentina, among other tectonic anomalies that occurs in this region of central Chile.

**ACKNOWLEDGMENTS.** This work was partially funded by projects FONDECYT-1950578, FONDEF-MI20 and ORSTOM.

## REFERENCES

- [1] DeMets, C., R. G. Gordon, D. F. Argus and S. Stein, Current plate motions, *Geophys. J. Int.*, **101**, 425-478, 1990.
- [2] Barazangi, M. B. and B. Isacks, Spatial distribution of earthquakes and subduction of the Nazca plate beneath South America, *Geology*, **4**, 686-692, 1976.
- [3] Bevis, M. and B. Isacks, Hypocentral trend surface analysis: Proving the geometry of Benioff zones, *J. Geophys. Res.*, **89**, 6153-6170, 1984
- [4] Cahill, T. and B. Isacks, Seismicity and shape of the subducted Nazca plate, *J. Geophys. Res.*, **97**, 17503-17529, 1992.
- [5] Swift, S. and M. Carr, The segmented nature of the Chilean seismic zone, *Phys. Earth Planet. Inter.*, **9**, 183-191, 1974.
- [6] Fuenzalida, A., M. Pardo, A. Cisternas, L. Dorbath, C. Dorbath, D. Comte and E. Kausel, On the geometry of the Nazca plate subducted under central Chile (32°-34.5°S) as inferred from microseismic data, *Tectonophys.*, **205**, 1-11, 1992.
- [7] Araujo, M. and G. Suárez, Geometry and state of stress of the subducted Nazca plate beneath central Chile and Argentina: evidence from teleseismic data, *Geophys. J. Int.*, **116**, 283-303, 1994.
- [8] Dewey, J. W., Seismicity studies with the method of Joint Hypocenter Determination, *Ph.D. Thesis, U. of California, Berkeley*, 1971.
- [9] Nábelek, J., Determination of earthquake source parameters from inversion of body waves, *Ph.D. Thesis, Mass. Inst. Technol., Cambridge*, 1984.
- [10] Suárez, G. and D. Comte, Comment on 'Seismic coupling along the Chilean subduction zone' by B. W. Tichelaar and L. R. Ruff, *J. Geophys. Res.*, **98**, 15825-15828, 1993.
- [11] Pacheco, J. F., L. R. Sykes and C. H. Scholz, Nature of seismic coupling along simple plate boundaries of the subduction type, *J. Geophys. Res.*, **98**, 14133-14169, 1993.
- [12] Tichelaar, B. W. and L. R. Ruff, Seismic coupling along the Chilean subduction zone, *J. Geophys. Res.*, **96**, 11997-12022, 1991.